Prediction of fruit texture with training population optimization for efficient genomic selection in apple

Morgane Roth[1], Mario Di Guardo[2,3], Walter Guerra[4], Hélène Muranty[5], Andrea Patocchi[1], Fabrizio Costa[2]

1. Plant Breeding Research Division, Agroscope, Wädenswil, Switzerland
2. Department of Genomics and Biology of Fruit Crops, Research and Innovation Centre, Fondazione Edmund Mach (FEM), Via E. Mach 1, 38010 San Michele all'Adige, Italy
3. Dipartimento di Agricoltura, Alimentazione e Ambiente, University of Catania, Catania, Italy
4. Research Centre Laimburg, Laimburg 6, 39040 Auer, Italy
5. IRHS, INRAE, Agrocampus-Ouest, Université d'Angers, SFR 4207 QuaSaV, Beaucouzé, France

Corresponding author: Morgane Roth, mroth@posteo.net, +33769852443

Further e-mails: Mario Di Guardo: mario.diguardo@unict.it ; Walter Guerra: walter.guerra@laimburg.it ; Hélène Muranty: helene.muranty@inra.fr ; Andrea Patocchi: andrea.patocchi@agroscope.admin.ch ; Fabrizio Costa: fabrizio.costa@fmach.it.

Date of submission: 02.12.2019
Number of tables: 3
Number of figures: 5, all on color-online only
Word count: 6,606
Number of supplementary tables: 7
Number of supplementary figures: 7

30 **Title**

31

32 Prediction of fruit texture with training population optimization for efficient genomic selection in apple

33

34 **Running title**

35 Genomic prediction for apple texture

36 **Keywords**

37 Apple, genomic prediction, rrBLUP, multi-trait, fruit texture, relatedness, training set

38 optimization

39 **Abbreviations**

Full name	Abbreviation
Acoustic Linear Distance	ALD
Acoustic Max Pressure	APMax
Acoustic Mean Pressure	APMean
Number of Acoustic Peaks	ANP
Bayesian Information Criterion	BIC
Best Linear Unbiased Predictor	BLUP
Collection	COLL
Discriminant Analysis of Principal Components	DAPC
Final Force	FF
Force Linear Distance	FLD
Initial Force	FI
Max Force	FMax
Mean Force	FMean
Single Nucleotide Polymorphism	SNP
Principal Component	PC
Principal Component Analysis	PCA
Number of Force Peaks	FNP
Test Set	TS
Training Set	TRS
Young Module	YM

40

41 **Highlight**

42 A genomic selection study, together with the optimization of the training set, demonstrated

43 the possibility to accurately predict texture sub-traits valuable for the amelioration of fruit

44 quality in apple.

45

46

2

Abstract

Texture plays a major role in the determination of fruit quality in apple. Due to its physiological and economic relevance, this trait has been largely investigated, leading to the fixation of the major gene PG1 controlling firmness in elite cultivars. To further improve fruit texture, the targeting of an undisclosed reservoir of loci with minor effects is compelling. In this work, we aimed to unlock this potential with a genomic selection approach by predicting fruit acoustic and mechanical features as obtained with a TA.XT*plus* texture analyzer in 537 individuals genotyped with 8,294 SNP markers. The best prediction accuracies following cross-validations within the training set (TRS) of 259 individuals were obtained for the acoustic linear distance (0.64). Prediction accuracy was further improved through the optimization of TRS size and composition according to the test set. With this strategy, a maximal accuracy of 0.81 was obtained when predicting the synthetic trait PC1 in the family 'Gala × Pink Lady'. We discuss the impact of genetic relatedness and clustering on trait variability and predictability. Moreover, we demonstrated the need for a comprehensive dissection of the complex texture phenotype and the potentiality of using genomic selection to improve fruit quality in apple.

Introduction

Fruits, during maturation and ripening, undergo a complex series of genetically programmed events contributing to their attractiveness and suitability for human consumption. Amongst the various physiological and physical changes, fruit texture is certainly the most important and investigated traits, especially in apple. A favorable texture is in fact highly appreciated by consumers, enabling, moreover, a long-term storage.

Texture can nowadays be dissected into two groups of sub-traits, mechanical and acoustic, contributing to distinguish between firm (based on mechanical sub-traits) and crispy (based on acoustic sub-traits) types of apples. These texture parameters have been already described and validated in apple (Costa *et al*., 2011, 2012), and were implemented in QTL-mapping studies carried out with bi-parental populations (Longhi *et al*., 2012) as well as more structured approaches, such as Pedigreed Based Analysis (PBA) and Genome-Wide Association Studies (GWAS, Kumar *et al*., 2013; Migicovsky *et al*., 2016; Amyotte *et al*., 2017; Di Guardo *et al*., 2017; McClure *et al.*, 2019). These works elucidated the complex genetic control of the fruit texture in apple, identifying a large number of QTLs distributed over the apple genome, with the most relevant regions located on chromosome 3, 10 and 16. This genetic complexity is moreover reflected in the regulation of the cell-wall and middle

81   lamella disassembling, a physiological process orchestrated by a myriad of cell-wall

82   modifying enzymes (Giovannoni, 2001; Costa *et al.*, 2010a). This highly polygenic control

83   can hamper the selection assisted by molecular markers in breeding activities programmed to

84   ameliorate fruit texture performance (Iwata *et al.* 2016). In the QTL mapping studies carried

85   out to date, a major region was located on chromosome 10, close to the polygalacturonase

86   locus (Costa *et al.*, 2010b; Longhi *et al.*, 2013). This QTL explains a high (about 40%) yet

87   incomplete part of the texture variance, leaving room for better harnessing this trait. As

88   introduced by Di Guardo *et al.* (2017), in modern breeding programs this locus has been fixed

89   through successive rounds of *ad-hoc* crossing and selection. In turn, the phenotypic variance

90   of modern families, obtained by crossing valuable parents for texture performance, might now

91   be under the control of other loci with minor-effect. Selection based on QTLs associated to

92   this trait can therefore be limited by the fact that QTL-based approaches ignore small effect

93   QTLs possibly underlying the control of such traits (Desta & Ortiz, 2014). To face this

94   limitation, an alternative approach for genome-assisted breeding known as genomic selection

95   (GS) has been introduced by the seminal work of Meuwissen *et al.* (2001). In contrast to

96   marker assisted selection, GS defines the estimation of the genetic merit of an individual

97   taking into account all genome-wide distributed genetic markers, making it especially relevant

98   for complex traits (Heffner *et al.*, 2009). GS considers two sets of individuals: the training set

99   (TRS), genotyped and phenotyped to train a prediction model, and the test set (TS, also called

100   validation set), represented by individuals only genotyped on which the genomic estimated

101   breeding value (GEBVs) is estimated (Heffner *et al.*, 2009; Crossa *et al.*, 2017). In principle,

102   the most favorable scenario for GS is to predict highly heritable traits in a TS highly related to

103   the TRS. While trait heritability can be increased (to a certain extent) by more precise and

104   more repeated phenotyping, relatedness between TS and TRS can be optimized with different

105   strategies. Dedicated approaches and tools have been proposed to address this issue based on

106   optimization parameters (Laloë, 1993; Rincent *et al.*, 2012; Isidro *et al.*, 2015) and algorithms

107   (Akdemir *et al.*, 2015). In theory, it could thus be feasible to acquire phenotypic and

108   genotypic data for a highly diverse TRS in the first place and, in the second place, to retain

109   individuals of the optimal TRS for a given TS *in silico*.

110   GS has been largely applied in major crops for primary traits such as yield (Crossa *et*

111   *al.*, 2017). In perennial species, GS would have a great potential in improving the breeding

112   efficiency due to their long generation time (McClure *et al.*, 2014). It has been pioneered in

113   forest trees (reviewed in Grattapaglia, 2017) and more recently in fruit trees such as crops

114   from the *Malus, Citrus and Pyrus* genera (Muranty *et al.* 2015; Minamikawa *et al.*, 2017,

4

115   2018). GS has also been recently employed to investigate fruit quality in tomato (Duangjit *et*

116   *al.*, 2016), while in apple standard fruit pomological traits were predicted using 8 to 20 full-

117   sib families as training populations (Kumar *et al.*, 2012, 2015; Muranty *et al.*, 2015). In apple,

118   low to high prediction accuracies were obtained depending on the cross-validation design and

119   on trait heritability. Among these studies, fruit texture was only partially addressed via

120   classical fruit firmness measurements (Kumar *et al.*, 2012, 2015; McClure *et al.*, 2018) and

121   sensorial evaluation (Kumar *et al.*, 2015).

122   In this work, we attempted to predict fruit texture in 6 full-sib families with a diverse

123   training set considering several acoustic and mechanical traits dissecting fruit texture. Further,

124   we explored the methodological improvements that can be made to optimize the TRS

125   according to the TS, which contributed to improve prediction accuracies. In this context, we

126   discussed the feasibility of genomic selection for ameliorating fruit quality through molecular

127   assisted breeding programs.

128

129   **Materials and methods**

130

131   *Plant Material*

132   The plant material and phenotyping strategies used in this work have been detailed in

133   previous works (Costa *et al.*, 2011; Longhi *et al.*, 2012; Di Guardo *et al.*, 2017). Briefly, two

134   types of plant materials have been used in this survey. The first was an apple collection

135   represented by 259 accessions planted in three replicates at the experimental orchards of the

136   Fondazione Edmund Mach (Trento) in the Northern part of Italy. The second type of plant

137   material consisted of 6 full-sib biparental families, for a total of 278 offsprings. Two ('FjDe':

138   'Fuji' x 'Delearly' and 'FjPL': 'Fuji' x 'Pink Lady') were located at the Fondazione Edmund

139   Mach (same orchard as the collection), while the other four ('GaPL': 'Royal Gala' x 'Pink

140   Lady', 'GaPi': 'Royal Gala' x 'Pinova', 'FjPi': 'Fuji' x 'Pinova' and 'GDFj': 'Golden

141   Delicious' x 'Fuji') were planted at the experimental orchard of the Laimburg Research

142   Center (Bolzano), located in the same area with near-identical climatic and pedological

143   conditions. At the time of the analysis, all plants (from both collection and families, together

144   named as 'population' here) were in a productive and adult phase. Fruit texture was

145   phenotyped in 2012, 2013 and 2015 for the collection, and in 2012 and 2013 for 'FjDe' and

146   'FjPL' and in 2012 and 2014 for the four remaining families (Table 1). Unlike the collection,

147   each offspring belonging to the six families was represented by a single tree (no replicates).

148   All plants, from both collection and bi-parental families, were grafted on 'M9' rootstock and

149 grown according to conventional horticultural management for plant training, pruning and

150 pest-disease control.

151   Fruits were harvested from each plant at the time of the physiological ripening stage,

152 established according to standard horticultural fruit quality parameters, such as the change in

153 color of the skin, seeds and flesh, fruit firmness value and the iodine coloration index

154 indicating the internal starch degradation. After harvest, fruits were stored for two months at

155 2°C with 95% of relative humidity.

156

157 *Texture phenotyping*

158   The texture performance of the apple fruit was phenotypically dissected into

159 mechanical and acoustic sub-traits with the use of a texture analyzer TA.XT*plus* (Stable

160 MicroSystems Ltd., Godalming, UK) equipped with an acoustic envelop device AED (Stable

161 MicroSystems Ltd., Godalming, UK), as described in Costa *et al.* (2011). For each genotype

162 included in the population, a homogeneous set of five apples was collected. Four identical

163 discs were isolated per fruit, avoiding seeds, seed cavity tissues or skin, for a total of 20

164 measurements per genotype (5 biological replicates and 4 technological replicates). Each

165 texture profile was then digitally elaborated identifying 12 texture measurements (*i. e.* 'sub-

166 traits'), four related to the acoustic performance and eight to the mechanical force-

167 displacement. In brief, the mechanical sub-traits were coded as: initial, final, maximum and

168 mean force (related to the different force values associated to the different parts of the force-

169 displacement profile), area, force linear distance (derived length of the profile), Young's

170 module (also known as elasticity module) and number of force peaks. The acoustic sub-traits

171 were maximum and mean acoustic pressure, acoustic linear distance and number of acoustic

172 peaks. A more exhaustive and complete description of the texture sub-traits is reported in

173 Costa *et al.* 2011.

174

175 *SNP genotyping*

176   The DNA employed for the genotyping of each individual considered in this survey

177 was isolated from young leaves collected at the beginning of the vegetative phase with the

178 Qiagen DNeasy Plant Kit and further quantified with a Nanodrop ND-8000

179 (ThermoScientific, USA). SNP markers were genotyped through the HiScan (Illumina, USA)

180 and the apple 20K SNP chip Infinium array (Illumina, USA) assembled within the framework

181 of the European project FruitBreedomics (Bianco *et al.*, 2014). The SNP pattern was initially

182 analyzed with the software GenomeStudio and further re-edited with ASSiST (Di Guardo *et*

6

183   *al.*, 2015). SNPs with minor allele frequencies lower than 0.05 and call rate below 0.2 were

184   filtered out with the package 'snpStats' (Clayton, 2019). The final set of markers successfully

185   recovered in the population consisted in 8,294 biallelic SNPs.

186   *Analysis of the fruit texture sub-traits*

187   We used a mixed linear model to get the best linear unbiased predictors (BLUPs) of

188   each individual's genotypic value. For each apple measured, we first calculated the mean over

189   the four technical replicates to retain only the biological replication level in the model. Each

190   of the twelve mechanical or acoustic sub-traits, considered as 'Y', was explained by the

191   genotype as random effect, the trial (location by year) as fixed effect and the random effect of

192   the error as: $Y_{i,j,k} = \mu + genotype_i + trial_j + e_{i,j,k}$ (1), with each phenotypic datapoint

193     $Y_{i,j,k}$ explained by the mean μ, the genotype i, the trial j and the error for each combination of

194   genotype, trial and replicate (k, *i.e.* a single apple). This model was fitted separately for all

195   traits with the 'lme4' R-package (Bates *et al.*, 2015). Broad-sense heritability was calculated

196   as $h^2 = \dfrac{\sigma_g^2}{\sigma_g^2 + \sigma_e^2/n_{rep}}$ (2), where σ_g^2 is the genotypic variance, σ_e^2 is the error variance and n_{rep}

197   the mean number of repetitions.

198   Principal component analysis (PCA) was performed on BLUPs with the 'FactorMiner'

199   R-package (Lê *et al.*, 2008). Only values from the collection were used to create the principal

200   components, while the families were plotted as supplementary individuals with principal

201   components (PC) coordinates calculated on the base of the PCs initially built with the

202   collection. Coordinates of individuals on the first and the second PCs ('PC1' and 'PC2') were

203   used for prediction and subsequently named 'synthetic' traits.

204

205   *Kinship and clustering analyses*

206   The realized additive relationship was calculated with the 'A.mat' function of the

207   'rrBLUP' package (Endelman, 2011) and depicted in a heatmap plot obtained with the R-

208   function 'heatmap.2' (package 'gplots', Warnes *et al.*, 2016). Genetic clustering was further

209   assessed in the collection with a discriminant analysis of principal components (DAPC,

210   Jombart *et al.*, 2010), carried out with the R-package 'adegenet' (Jombart, 2008) using the

211   entire set of 8,294 markers. In the first step, six significant clusters were retained with the

212   function 'find.clusters' using 300 principal components and selecting the number of clusters

213   with the highest likelihood (based on the Bayesian information criterion value-BIC, Fig. S1).

214   Out of these variables, 150 were retained and employed in the clustering computed with the

<p style="text-align:center">7</p>

215 'dapc' function, which created five principal components that maximized the inter-cluster

216 distance while minimizing the inter-individual distance within each cluster. The assignment of

217 offsprings to clusters was obtained with the function 'predict_dapc'. Pairwise Fst values

218 between clusters were then computed with the entire SNP set with the function

219 'pairwise.WCfst' from R-package 'hierfstat' (Yang, 1998, Goudet 2005).

220

221 *Prediction models*

222   Genomic predictions were computed through two models implemented in the rrBLUP

223 framework, as reported in Endelman *et al.* 2011 (and 'rrBLUP R'-package):

224

225        $Y = \mu + Zu + e$ (3), model A

226        $Y = \mu + X\beta + Zu + e$ (4), model B

227

228 where Y is the vector of BLUPs of the genotypic values ($n \times 1$), μ is the mean of the

229 phenotype, W is the $n \times p$ incidence matrix linking the genotypes to observations of Y, G

230 contains the allelic states of the marker loci (additive coding -1,0,1), u the $p \times 1$ vector of

231 random marker effects with $u \sim N(0, I\sigma_u^2)$, and e is a $n \times 1$ vector of random errors. Model

232 (B), contains also X, the $n \times c$ incidence matrix for cluster assignment of each individual,

233 where c is the number of clusters and β is the $c \times 1$ vector of the cluster fixed effects.

234   A 5-fold cross-validation was applied within the collection with both model (A) and

235 (B) respectively and repeated 100 times. For predicting each family (considered then as TS),

236 three different TRS composition rules, named as "scenarios", were tested using the two

237 models *without a priori genetic information on individuals*. In scenario 1, each family was

238 predicted using the collection only. In scenario 2, 30% of individuals of the predicted family

239 were instead added to the collection in the TRS while the remaining 70% formed the TS. In

240 scenario 3, a single half-sib family (*e.g.* 'GaPL' is half-sib with 'FjPL' and 'GaPi') was added

241 to the collection to form the TRS, leading to two to four TRS possibilities (and accuracy

242 values). To illustrate the scenarios taking 'GaPi' as an example, scenario 1 corresponded to

243 [TRS = COLL // TS = 'GaPi'] (one accuracy estimation only), scenario 2 corresponded to

244 [TRS = 30% 'GaPi' offsprings + COLL // TS = 70 % remaining offsprings of 'GaPi']

245 (sampling of the 30% repeated 100 times, giving 100 estimations of the accuracy), and

246 scenario 3 corresponded to [TRS = 'GaPL' *or* 'FjPi' + COLL // TS = 'GaPi'] (resulting here

247 in the estimation of two accuracy values).

248   TRS optimization was then performed *with a priori genetic information on individuals*
249   by varying TRS size with different optimization methods relying on the prediction model A.
250   To this end, a relatedness-driven and a principal component-driven approaches were adopted.
251   The relatedness-driven approach was tested in three different manners: (i) by starting with the
252   10 most-related individuals and adding single individuals with decreasing mean relationship
253   to the family, or (ii) with decreasing maximum relationship to the family (N=10 to N=259), or
254   (iii) by starting with a TRS composed of the most related cluster and adding less and less
255   related clusters successively (final TRS size N=259). In the principal component-driven
256   approach, TRS individuals were selected with increasing TRS size using a protocol by
257   Akdemir (R-package 'STPGA', 2019). The optimal TRS with increasing size from 10
258   individuals to 259 with increments of 20 individuals was chosen based on the five principal
259   components obtained with DAPC analysis and using the 'CDmean' design criteria and the
260   function 'GenAlgForSubsetSelection'. Here, individuals were chosen independently for each
261   TRS size, meaning that we did not proceed to a gradual enrichment of the TRS.

262   All accuracy values were based on Pearson correlation calculated between observed
263   values (*i.e.* BLUPs of genotypic values) and predicted values of the TS individuals. When
264   standard deviations were not available, we calculated an approximate 95% confidence interval
265   of the correlation coefficient with a Fisher's Z-transformation ('cor.test' function in base R).
266   Calculations were performed in R (R Core Team, 2014) and graphs were created with the R-
267   package 'ggplot2' (Wickham, 2016).

268   **Results**

269
270   *Fruit texture phenotypic dissection*

271   The fruit texture phenotypic data used in this survey were represented by the analysis
272   of multi-trait features accurately dissected into 4 acoustic and 8 mechanical sub-traits (Table
273   2, Table S1). A mixed linear model was used to obtain BLUPs of genotypic values used in the
274   further analyses. The texture sub-traits showed an overall high heritability, spanning from
275   0.90-0.96 for the entire population (collection and families) to 0.88-0.94 for the apple
276   accessions included in the collection (Table 2). In order to visualize the diversity and
277   inheritance of fruit texture profiles, a principal component analysis (PCA) was performed
278   using the twelve textural sub-traits measured in the collection, while individuals from families
279   were considered as supplementary individuals (see also Di Guardo et al. 2017, Fig. 1). In this
280   analysis, the first PC axis (PC1), explaining 80.5% of phenotypic variability, comprehensively
281   summarizing the general variability of the twelve phenotypic variables. The second axis

9

282   (PC2), instead, mainly differentiated the acoustic from mechanical sub-traits, explaining a

283   smaller, yet substantial, portion of the phenotypic variability (12.7%, Fig. 1A).

284   In the distinction between the two types of texture sub-traits (mechanical and acoustic)

285   by PC2, it is worth noting that one mechanical variable (FNP) was oriented together with the

286   acoustic group. FNP was in fact more correlated with acoustic sub-traits (mean correlation

287   0.77) than with the rest of the mechanical ones (mean correlation 0.69, Fig. 1A). Individuals

288   of the population were present in the four quadrants of the PCA 2D-plot, identifying different

289   types of texture: mealy (negative PC1), predominantly firm (positive PC1 and negative PC2)

290   and predominantly crispy (positive PC1 and positive PC2, Fig. 1B). With this regard, the

291   distribution of texture profiles indicated that the collection is mainly composed of individuals

292   with low to moderate crispiness and firmness at the exception of few outliers. It is also

293   important to note that variation on the PC2 axis is much lower for accessions having a

294   negative PC1 value, illustrating that mealy apples cannot be crispy (Fig. 1B).

295   The six parental cultivars, known to have different texture profiles after two months of

296   storage, were, as expected, plotted over the different quadrants of the PCA 2D-plot (Fig. 1C).

297   'Delearly' and 'Golden Delicious' were plotted in the area corresponding to the mealy type of

298   apple, while 'Royal Gala' was instead grouped with moderately firm apples. 'Fuji', 'Pink

299   Lady' and 'Pinova' were instead positioned in the positive quadrant for both PC1 and PC2,

300   corresponding to the crispy type of apple. The populations originated by the controlled cross

301   of these varieties were also distributed over the PCA plot with specific orientations (Fig. 1B-

302   C). In particular, 'FjPL' offsprings were mostly projected towards the 'firm quadrant', while

303   'GDFj' was more oriented in the 'crispy quadrant' (Fig. 1B). Moreover, the segregation of the

304   families was very variable with regard to their corresponding parental profiles (Fig. 1C).

305   While 'GDFj' was the only family showing a classic type of segregation (intermediate

306   between the parents), the distributions of the other families were more similar to one of the

307   two parents ('FjDe' and 'GaPi'), with a varying number of offsprings being of transgressive

308   type ('FjDe' ,'GaPL', 'FjPi' and 'FjPL'). In particular, while 'Fuji' and 'Pink Lady' showed a

309   very similar texture profile on PC1 (2.99 and 3.14 respectively), major differences were

310   observed on the PC2 (1.6 and 0.51 respectively, Fig. 1C, Table S1). Variation in the texture

311   performance of 'FjPL' offsprings was also observed on the PC2 axis, although with a much

312   broader variation with regards to 'Fuji' and 'Pink Lady'. Accordingly, apples of this family

313   were overall firm to very firm while having a very low to very high crispiness (Fig. 1C, Table

314   S1, Fig. S2).

315

10

316   *Additive relationship and genetic clustering in the population*

317   The accuracy of genomic prediction is highly correlated to the level of relatedness

318   between the training and the test sets (TRS and TS). To identify the overall patterns of

319   relatedness between families and the collection, a clustering analysis of all the individuals

320   based on their pairwise additive relationship was performed (Fig. 2). The parental cultivar

321   'Royal Gala' was found to be the most related to the rest of the collection (mean additive

322   relatedness -6.32E-4), while 'Fuji' was the most distantly related (mean additive relatedness -

323   0.102, Table S2). Accordingly, 'Royal Gala'–related families were more closely related to the

324   collection respect to the four 'Fuji'-related families, plotted together on the top-right panel of

325   the heatmap (Fig. 2). Mean additive relationship values for each family reflected the patterns

326   observed on the heatmap, namely higher values for 'GaPi' and 'GaPL' (-0.021 to -0.020) and

327   lower for 'Fuji'-related families (-0.056 to -0.078, Table 1, Table S2).

328   To investigate the genetic structure of the collection and its impact on the prediction

329   accuracy, a discriminant analysis of principal component with the entire SNP set (8,294

330   SNPs) was performed. Through the BIC criteria, six clusters, described with five principal

331   components, were defined as the most probable (see Methods, Fig. S1). All parental cultivars

332   were assigned to cluster 5, except 'Fuji' that was grouped in cluster 2 (Fig. 3A, Table S3). Of

333   these clusters, cluster 5 resulted to be the largest (N=66), while the smallest was cluster 6

334   (n=25, Table 1, Table S3). The cluster assignment in families was predicted using the

335   principal components derived by the DAPC analysis carried out on the collection. Most of the

336   individuals were assigned to the parental clusters 2 and 5, while 8 individuals of 'FjDe' and

337   one of 'FjPi' were assigned to cluster 1 (Table 1, Fig. 3B-C). Overall, clusters 2 and 5

338   contained the largest part of the whole population, while clusters 1, 3, 4 and 6 were the lowest

339   represented (Fig. 3C, Table S3). However, while the DAPC analysis suggested this genetic

340   clustering as the most realistic in the diversity panel represented by the collection, the

341   pairwise Fst-values between clusters indicated a low genetic differentiation (values comprised

342   between 0.002 and 0.018, Table S4). The Fst value between clusters 2 and 5, containing the

343   parents and most of their offsprings, was for instance 0.013. As our design allowed the

344   comparison of families obtained from crosses within cluster 5 ('Royal Gala'-related) and

345   between clusters 2 and 5 ('Fuji'-related), the information on genetic clustering was further

346   used to control the genetic background in the subsequent prediction models ('model B', see

347   Methods). The phenotypic distributions across clusters reveal that clusters 2 and 5 have, for

348   all traits except PC2, elevated values compared to other clusters, with values of cluster 2

11

349   individuals surpassing those of cluster 5 (Fig. S3), indicating a possible correlation existing

350   between genetic clustering and texture.

351

352   *Cross-validations within collection*

353   A hundred 5-fold cross-validations within the collection were run with the additive

354   rrBLUP model on BLUPs with and without considering the genetic clustering as a fixed effect

355   (models A and B, respectively). In this context, PC1 and PC2 were also considered as traits,

356   leading in the end to 14 predicted traits (Fig. S4). Instead of improving predictions, the

357   inclusion of the clustering effect degraded accuracies for all traits, with a maximum accuracy

358   decrease of 0.02 for the mean force (FMean). The highest mean prediction was obtained for

359   the acoustic linear distance (ALD, $mean\ cor = 0.64$, Fig. S4) whereas the number of force

360   peaks yielded the second highest accuracy (FNP, $mean\ cor = 0.63$, Fig. S4, Table S5).

361   Moreover, while FNP yielded a relatively high accuracy as inferred from heritability (0.93,

362   Table 2), the overall mean accuracies among traits did not follow the ranking of heritability

363   obtained within the collection phenotypes (Wilcoxon signed-rank-test, p-value = 4.88E-4,

364   model A).

365

366   *Genomic prediction of families without training population optimization*

367   In practice, families can be predicted with any available related genetic material that

368   has been genotyped and phenotyped. For this reason, three different scenarios of training

369   population design were tested, including or not individuals from the predicted family or from

370   a half-sib family (see Methods, "Prediction models"). The predictions in each of these

371   scenarios were calculated with the two prediction models (A and B, respectively depicted in

372   Fig. 4, Fig. S5). Without clustering, overall three families ('FjPi', 'GaPi' and 'GaPL') could

373   be predicted with moderate to high accuracies (accuracies ranging from 0.08 for PC2 in

374   'GaPi' to 0.73 for PC1 in 'GaPL', respectively), with PC1 being the best predicted trait

375   among these families (mean for scenario 1, model A: 0.50, Fig. 4). The three remaining

376   families yielded near-zero ('FjPL') or negative accuracies ('FjDe' and 'GDFj', mean

377   accuracies between -0.29 and 0.30, Fig. 4). The correlations between predicted and observed

378   values for each individual and for all traits and families obtained are depicted in Fig. S6

379   (model A and scenario 1). Out of 252 combinations of trait, scenario and family predictions,

380   only 74 gave better accuracies (considering an increase in accuracy larger than 0.01). When

381   considering accuracies above 0.20, this number dropped to 40 out of 103 family-trait-scenario

12

382 combinations (maximum gain: 0.04, Table S6, Fig 4, Fig. S5). Thus, the implementation of
383 clustering did not clearly improve the predictions of families.

384   It is also important to underline that the addition of related individuals to the collection
385 did not systematically improve the predictions. For instance, in 'GaPL' the prediction was
386 more accurate with scenario 1 with regards to scenario 2 and 3 (mean prediction accuracies of
387 0.60, 0.56 and 0.53 respectively for scenario 1, 2, 3, respectively, model A). Scenario 2
388 particularly improved the accuracies in 'FjPi' (mean accuracies of 0.32, model A) as it better
389 predicted 12 out of 14 traits. Scenario 3 instead was the lowest performing, although it
390 increased the prediction accuracy of 7 traits (8 with clustering) in 'GaPi' (mean accuracy of
391 0.38, all values across trait in model A, Fig 4, Table S6).

392

393 *Genomic prediction of families with training population optimization*

394   To test the hypothesis that retaining only the most related individuals or clusters in the
395 TRS might allow to maximize prediction accuracies, we compared the predictive abilities
396 obtained for each family and trait using training sets with different sizes. This process started
397 with a small TRS having the highest relatedness to which individuals were added in the order
398 of decreasing relatedness to reach the size of the entire collection using three different
399 enrichment procedures (see Methods). TRS optimization was also carried out with a more
400 sophisticated approach based on the optimization algorithm presented by Akdemir *et al.*
401 (Akdemir *et al.*, 2015; Akdemir & Isidro-Sánchez, 2019), using DAPC-defined principal
402 components and the 'CD-Mean' value as decision criterion. The results obtained using these
403 different methods are illustrated in Table 3, Fig. 5 and Fig. S7 for four traits selected for their
404 practical relevance (ALD, FNP, PC1 and PC2) while results for the remaining traits are
405 reported in Table S7. Regarding the four selected traits, the best accuracy for each of the
406 6×4 family-trait combinations was in most cases obtained with the addition of single
407 individuals based on their relationship to the family (in 10 cases using the maximum
408 relationship and in 10 cases using the mean relationship, Fig. 5A and B, Table 3, Table S7).
409 The mean optimal population size was 92 individuals with a minimum size of 10 and a
410 maximum size of 202 individuals (Table 3, Table S7), meaning that the entire collection was
411 never considered as the optimal TRS for predicting texture. The maximal accuracies observed
412 ranged from 0.01 to 0.81, which corresponded to a mean increase in accuracy of 0.17 when
413 compared to predictions of families with the entire collection (minimum increase: 0.02;
414 maximum increase: 0.40 – compared to scenario 1, model A). The highest accuracy was 0.81,

13

415 and was obtained for the "multi-trait" PC1 in 'GaPL' family with only 129 individuals, *i.e.*

416 nearly half of the collection size. The distribution of accuracies with increasing TRS size in

417 each family for the four focal traits was also investigated (Fig. 5). Overall, traits tended to

418 follow the same trend within a family. In families 'GaPL' and 'GaPi', which had the highest

419 relatedness to the collection among all families (Table 1), the accuracy was moderate to high

420 from as few as 100 individuals for ALD, FNP and PC1, and remained relatively stable while

421 increasing TRS size (Fig. 5A-D). 'FjPi' was the only family for which increasing TRS up to

422 200 individuals resulted in a clear accuracy improvement, with any of the approaches

423 implemented here (Fig. 5A-D). In families with overall low accuracies, such as 'FjDe', 'FjPL'

424 and 'GDFj', the highest accuracy was in most cases obtained with 10 to 70 individuals, and

425 declined or remained stable with larger TRS size (Fig. 5A-D). In 'GDFj', for instance,

426 accuracies above 0.2 were found only with a TRS of 10 to 66 individuals (Fig. 5A-C, Table

427 S7). Moreover, while FNP was not predictable in 'GDFj' with the entire collection ($cor =$

428 0.08 for $N = 259$), an improved accuracy of 0.32 was observed with as few as 15 individuals

429 (based on maximum relationship, Fig. 5B).

430 **Discussion**

431   In this work we assessed the feasibility of genomic selection (GS) for apple texture by

432 performing an in-depth analysis of this complex phenotype together with the genetic

433 correlates influencing its genomic predictions. The results presented here on genomic

434 prediction for apple texture evidenced a large potential for GS for this trait, providing

435 important key elements and tools to set-up a prediction experiment given the available genetic

436 information in any apple population.

437

438 *Family-dependent fruit texture profiles and fruit texture prediction*

439   The texture dissected "sub-traits" were highly heritable, although variability within

440 families was very contrasted, showing, in specific cases, a transgressive segregation, such as

441 'FjPL'. Although the traits were predictable with moderate to high accuracy within the

442 collection (accuracies between 0.41 and 0.64), this was not easily achievable in all biparental

443 families. Without TRS optimization, texture could be accurately predicted for 'GaPL' (mean

444 accuracy of 0.57), while 'GaPi' and in 'FjPi' showed a moderate prediction accuracy (mean

445 accuracy of 0.30). In contrast, near-zero or negative accuracies were instead obtained for

446 'FjDe', 'FjPL' and 'GDFj' across traits (mean accuracy of -0.05). Surprisingly, large negative

447 accuracy values were repeatedly obtained in 'FjDe' and 'GDFj', which could be potentially

448 explained by the strong epistatic effect possibly present in these families (Lehner, 2011) or by

14

449 a systematic bias due to the calculation of the Pearson correlation coefficient (Zhou *et al.*,

450 2016), indicating that fruit texture cannot be predicted in these families using the entire

451 collection as TRS. In contrast, previous works on firmness and crispiness yielded mostly low

452 accuracies when predicting unobserved genotypes in a set of families or in a collection

453 (between 0.15 and 0.35, Kumar *et al.* 2015, McClure et al. 2018). A much higher accuracy of

454 0.83 was found for firmness by Kumar *et al.* (2012), which can be mainly explained by their

455 crossing design and validation procedure. In the present study, the analysis of PCA allowed to

456 better understand the relation between firmness and crispiness, both positively correlated and

457 summarized by PC1 and PC2, with PC2 specifically dissecting the difference between these

458 two texture sub-traits. When used as synthetic trait in the computation, PC1 was among the

459 best predictable traits (accuracy of 0.59 in collection and highest accuracy among traits and

460 family: 0.73 in GaPL), justified by the 80.5% of total phenotypic variation explained by PC1,

461 while PC2 accounted only for 12.7%. Despite the lower variability of PC2, this trait could be

462 predicted with a reasonable accuracy of 0.42 in the collection, while in most of the families

463 the accuracy level was above 0.2 (with, and in some cases without TRS optimization). PC2

464 was not predictable in 'GDFj' and 'FjPL', two families with moderate and high transgression

465 on the PC2 axis. The results showed that using PC1 and PC2 as a first tentative to perform a

466 multi-trait prediction was a relevant method to predict fruit texture profiles through an

467 integrative approach.

468

469 *Impact of genetic clustering and relatedness on prediction accuracy*

470 Having highly related individuals between the TRS and the TS is necessary but not

471 always sufficient for an optimal TRS design; in fact enlarging the TRS with scarcely related

472 individuals can diminish prediction accuracies (Lorenz & Smith, 2015). Moreover, trait

473 variation can be coupled with genetic structure. Several studies have for instance showed the

474 impact of genetic structure on genomic prediction, demonstrating that taking genetic structure

475 into account can improve GS efficiency (Guo *et al.*, 2014; Isidro *et al.*, 2015; Rio *et al.*,

476 2019). Although in apple the genetic structure is known to be weak, with substantial levels of

477 admixture in apple cultivars (Urrestarazu *et al.*, 2016; Vanderzande *et al.*, 2017; Cornille *et*

478 *al.*, 2019), it could still have a relevant effect on predictions, depending on the population

479 composition and the trait under investigation. Significant genetic structure has been identified,

480 for instance, between dessert and cider apples, which could potentially be correlated with fruit

481 quality traits (Lassois *et al.*, 2016). Through the implementation of the DAPC method, six

482 significant although lowly differentiated genetic clusters were obtained, with families

15

483   belonging to one or two specific clusters, depending mostly to the assignment of their parental

484   cultivars. While some degree of correlation was apparent between the genetic clustering of

485   individuals and their phenotypic distribution (Fig. S3), the addition of the clustering effect

486   into the prediction model almost systematically degraded the prediction accuracies. Moreover,

487   the TRS optimization based on clustering was the lowest performing among the four methods

488   tested. This could indicate that additive relationship alone already captured the genetic

489   clustering present in our population. One important information given by the clustering

490   patterns was that the 'GaPL' and 'GaPi' families, for which both parents were in the same

491   genetic cluster or in the best represented cluster in the collection (Cluster 5), yielded the best

492   predictions.

493   The genetic parameter having the largest impact on predictions was genetic

494   relatedness, with the two families most related to the collection ('GaPL' and 'GaPi') yielding

495   by far the highest accuracies compared to the remaining Fuji-related families. This

496   observation finds consistency to the fact that genetic relationship is a fundamental parameter

497   in genomic prediction (see *e.g.* Habier *et al.*, 2010; Clark *et al.*, 2012; Daetwyler *et al.*, 2014).

498   The addition of closely-related individuals from the same family (scenario 2) or from a

499   complete half-sib family (scenario 3) to the collection did not improve the prediction

500   accuracy, except for 'FjPi', for which scenario 2 was the most accurate. This result might

501   indicate that either the collection retains already 'enough' diversity to predict families, or that

502   the excess of unrelated individuals in the collection cannot be corrected by adding related

503   individuals. Thus, scenario 2 and 3 do not seem to effectively improve the TRS.

504   To this end, the gradual increase of the TRS size using *a priori* information of genetic

505   parameters was used as an alternative optimization strategy. TRS optimization was tested in

506   four different ways, based on *a priori* information on similarities between individuals. These

507   were represented either by additive relationship or by genetically derived principal

508   components coordinates (Fig. 5, Fig. S7, Table 3, Table S7). The results allowed in all cases

509   to improve predictions tested beforehand with TRS scenarios 1 to 3 with a minimal increase

510   of 0.2 and maximal increase of 0.4, reaching a maximum accuracy of 0.81 ('GaPL', PC1,

511   Table 3). This means that the maximum accuracies were also never reached by employing the

512   entire collection, especially for families with the lowest genetic relatedness to the TRS (*i.e.* to

513   the collection here). The best prediction accuracy for fruit texture in apple was obtained with

514   the implementation of 50 individuals in the TRS for families less related to the entire TRS and

515   at least 100 accessions for families with a higher genetic relationship (or clustering within the

516   major genetic cluster of the TRS, such as 'GaPL' and 'GaPi' here). These results are

16

517 consistent with previous findings in barley from Lorenz and Smith (2015), that showed the
518 detrimental effects of adding unrelated individuals to the TS into the TRS, partially
519 contradicting the idea that having at least one related individual in the TRS is sufficient to
520 increase accuracies (Daetwyler *et al.*, 2014).

521 Our results thus provided useful information for the TRS composition, illustrating the
522 complex roles of structure and relatedness in shaping texture variability in apple.

523

524 *Towards a simplified assessment of fruit texture for genomic selection*

525 The improvement of fruit texture is still limited by the time-consuming and expensive
526 assessment needed for its dissection and the low variation observed in modern elite apple
527 accessions due to the fixation of PG1 (Atkinson *et al.*, 2012; Di Guardo *et al.*, 2017). Thus,
528 even though we demonstrate the feasibility of GS for apple texture, its application will be
529 considered only if predictions are precise enough to perform the costly phenotyping of the
530 TRS. The characterization of texture is a challenging task, as this trait is composed of
531 mechanical and acoustic sub-traits. The analysis of PC1 and PC2 relied on the texture
532 dissection and the measurements of these 12 traits. In particular, FNP, which is the number of
533 mechanical peaks observed in the mechanical profile generated by fruit compression on the
534 texture analyzer, was highly correlated with the group of the acoustic traits related to
535 crispiness. As mechanical traits are easier to measure than acoustic ones, FNP would be in
536 practice the best measurement to choose for assessing crispiness. Since we also obtained high
537 prediction accuracy for FNP (0.63 in collection and maximum of 0.78 in "optimized" family
538 prediction), we propose this sub-trait as the most valuable descriptor for fruit texture,
539 minimizing the effort needed to phenotype such as complex phenotype. Moreover, the
540 predictions presented in this study have been performed with a set of 8,294 SNPs, which is
541 still not dense enough considering the rapid decay of the linkage disequilibrium in apple
542 (Laurens *et al.* 2018). Although we reached already satisfying accuracies with this amount of
543 SNP, it would be useful to increase the number of markers with the available apple 480K
544 (Bianco *et al.*, 2016) or by using genotyping-by-sequencing methods (Gardner *et al.*, 2014) to
545 further improve predictions.

546 The use of principal component as synthetic traits resulted to be a valuable multi-trait
547 approach to better predict and understand the texture variability. Here, we investigated in
548 details that fruit crispiness (PC2) in particular is less variable than fruit firmness (PC1). While
549 crispy apples are necessarily firm, the opposite relationship is in fact not validated. Our
550 predictions indicated that fruit firmness in apple can be accurately selected (along PC1), but it

17

551   needs to be taken into account that an excessive value for this trait can lead to unpleasant

552   quality perception for the consumer. On the other side, crispiness was better predicted with

553   the PC2. Despite the lower variation for crispiness in our population, the selection for this trait

554   resulted to be feasible, although with lower accuracy. To improve the predictions for

555   crispiness we might need to increase the variability for this trait within the TRS. More

556   generally, while the selection on fruit traits has shaped apple domestication, the current

557   cultivated pool relies on a few founders, hence having a narrow genetic basis. Thus, a better

558   targeting of apple texture might necessitate a pre-breeding step incorporating or generating

559   genetic diversity for this trait with the use of mealy cultivars and of wild relatives of *Malus*

560   *domestica* (Khan *et al.*, 2014; Peace *et al.*, 2019).

561

562   **Supplementary data**

563   **Table S1**. Texture genotypic values and coordinates for PC1 and PC2.

564   **Table S2**. Additive relationship matrix.

565   **Table S3**. Assignments of individuals to genetic clusters.

566   **Table S4**. Pairwise Fst-values between genetic clusters.

567   **Table S5**. Accuracies obtained in cross-validations within the collection using two models.

568   **Table S6**. Accuracies obtained in family predictions using two models and three TRS

569   scenarios.

570   **Table S7**. Accuracies obtained in family predictions with TRS optimization with four

571   methods.

572   **Fig. S1**. Bayesian information criterion values obtained in the discriminant analysis of

573   principal components.

574   **Fig. S2**. Distribution of texture genotypic values according to the type of population.

575   **Fig. S3**. Distribution of texture genotypic values according to cluster assignments.

576   **Fig. S4**. Accuracies obtained from cross-validations within the collection.

577   **Fig. S5**. Accuracies obtained for each family in three prediction scenarios with model B.

578   **Fig. S6**. Observed vs. predicted values in predictions for each family on each trait with model

579   A.

580   **Fig. S7**. Comparison of methods for the optimization of the training population.

581

582   **Acknowledgements**

585   (www.FruitBreedomics.com). The views expressed in this work are the sole responsibility of

586   the authors and do not necessarily reflect the views of the European Commission.

References

Akdemir D, Isidro-Sánchez J. 2019. Design of training populations for selective phenotyping in genomic prediction. *Scientific Reports* **9**: 1446.

Akdemir D, Sánchez JI, Jannink J-L. 2015. Optimization of genomic selection training populations with a genetic algorithm. *Genetics Selection Evolution* **47**: 38.

Amyotte B, Bowen AJ, Banks T, Rajcan I, Somers DJ. 2017. Mapping the sensory perception of apple using descriptive sensory evaluation in a genome wide association study. *PLoS ONE* **12**: e0171710.

Atkinson RG, Sutherland PW, Johnston SL, Gunaseelan K, Hallett IC, Mitra D, Brummell DA, Schröder R, Johnston JW, Schaffer RJ. 2012. Down-regulation of POLYGALACTURONASE1 alters firmness, tensile strength and water loss in apple (*Malus × domestica*) fruit. *BMC Plant Biology* **12**: 129.

Bates D, Mächler M, Bolker B, Walker S. 2015. Fitting linear mixed-effects models using lme4. *Journal of Statistical Software* **67**.

Bianco L, Cestaro A, Linsmith G, *et al.* 2016. Development and validation of the Axiom ® Apple480K SNP genotyping array. *The Plant Journal* **86**: 62–74.

Bianco L, Cestaro A, Sargent DJ, *et al.* 2014. Development and validation of a 20K single nucleotide polymorphism (SNP) whole genome genotyping array for apple (*Malus × domestica* Borkh). *PLoS ONE* **9**: e110377.

Clark SA, Hickey JM, Daetwyler HD, van der Werf JHJ. 2012. The importance of information on relatives for the prediction of genomic breeding values and the implications for the makeup of reference data sets in livestock breeding schemes. *Genetics Selection Evolution* **44**: 4.

Clayton D. 2019. snpStats: SnpMatrix and XSnpMatrix classes and methods. R package version 1.36.0. doi: 10.18129/B9.bioc.snpStats.

Cornille A, Antolín F, Garcia E, Vernesi C, Fietta A, Brinkkemper O, Kirleis W, Schlumbaum A, Roldán-Ruiz I. 2019. A multifaceted overview of apple tree domestication. *Trends in Plant Science* **24**: 770–782.

Costa F, Alba R, Schouten H, *et al.* 2010a. Use of homologous and heterologous gene expression profiling tools to characterize transcription dynamics during apple fruit maturation and ripening. *BMC Plant Biology* **10**: 229.

Costa F, Cappellin L, Fontanari M, Longhi S, Guerra W, Magnago P, Gasperi F, Biasioli F. 2012. Texture dynamics during postharvest cold storage ripening in apple (*Malus × domestica* Borkh.). *Postharvest Biology and Technology* **69**: 54–63.

Costa F, Cappellin L, Longhi S, *et al.* 2011. Assessment of apple (*Malus × domestica* Borkh.) fruit texture by a combined acoustic-mechanical profiling strategy. *Postharvest Biology and Technology* **61**: 21–28.

Costa F, Peace CP, Stella S, Serra S, Musacchi S, Bazzani M, Sansavini S, Van de Weg WE. 2010b. QTL dynamics for fruit firmness and softening around an ethylene-dependent polygalacturonase gene in apple (*Malus × domestica* Borkh.). *Journal of Experimental Botany* **61**: 3029–3039.

Crossa J, Pérez-Rodríguez P, Cuevas J, *et al.* 2017. Genomic selection in plant breeding: methods, models, and perspectives. *Trends in Plant Science* **22**: 961–975.

Daetwyler HD, Bansal UK, Bariana HS, Hayden MJ, Hayes BJ. 2014. Genomic

prediction for rust resistance in diverse wheat landraces. *Theoretical and Applied Genetics* **127**: 1795–1803.

Desta ZA, Ortiz R. 2014. Genomic selection: genome-wide prediction in plant improvement. *Trends in Plant Science* **19**: 592–601.

Duangjit J, Causse M, Sauvage C. 2016. Efficiency of genomic selection for tomato fruit quality. *Molecular Breeding* **36**: 1–16.

Endelman JB. 2011. Ridge regression and other kernels for genomic selection with R package rrBLUP. *The Plant Genome Journal* **4**: 250.

Gardner KM, Brown P, Cooke TF, Cann S, Costa F, Bustamante C, Velasco R, Troggio M, Myles S. 2014. Fast and cost-effective genetic mapping in apple using next-generation sequencing. *G3 (Bethesda)* **4**: 1681–1687.

Giovannoni J. 2001. Molecular biology of fruit maturation and ripening. *Annual Review of Plant Physiology and Plant Molecular Biology* **52**: 725–749.

Grattapaglia D. 2017. Status and perspectives of genomic selection in forest tree breeding. In: Varshney R, Roorkiwal M, Sorrells M, eds. *Genomic selection for crop improvement*. Cham: Springer, 199–249.

Di Guardo M, Bink MCAM, Guerra W, *et al.* 2017. Deciphering the genetic control of fruit texture in apple by multiple family-based analysis and genome-wide association. *Journal of Experimental Botany* **68**: 1451–1466.

Di Guardo M, Micheletti D, Bianco L, *et al.* 2015. ASSIsT: an automatic SNP scoring tool for in- and outbreeding species. *Bioinformatics*: btv446.

Guo Z, Tucker DM, Basten CJ, Gandhi H, Ersoz E, Guo B, Xu Z, Wang D, Gay G. 2014. The impact of population structure on genomic prediction in stratified populations. *Theoretical and Applied Genetics* **127**: 749–762.

Habier D, Tetens J, Seefried F-R, Lichtner P, Thaller G. 2010. The impact of genetic relationship information on genomic breeding values in German Holstein cattle. *Genetics Selection Evolution* **42**: 5.

Heffner EL, Sorrells ME, Jannink J-L. 2009. Genomic selection for crop improvement. *Crop Science* **49**: 1.

Isidro J, Jannink J-L, Akdemir D, Poland J, Heslot N, Sorrells ME. 2015. Training set optimization under population structure in genomic selection. *Theoretical and Applied Genetics* **128**: 145–158.

Iwata H, Minamikawa MF, Kajiya-Kanegae H, Ishimori M, Hayashi T. 2016. Genomics-assisted breeding in fruit trees. *Breeding Science*, **66**: 100-115.

Jombart T. 2008. adegenet: a R package for the multivariate analysis of genetic markers. *Bioinformatics* **24**: 1403–1405.

Jombart T, Devillard S, Balloux F. 2010. Discriminant analysis of principal components: a new method for the analysis of genetically structured populations. *BMC Genetics* **11**: 94.

Khan MA, Olsen KM, Sovero V, Kushad MM, Korban SS. 2014. Fruit quality traits have played critical roles in domestication of the apple. *The Plant Genome* **7**.

Kumar S, Chagné D, Bink MCAM, Volz RK, Whitworth C, Carlisle C. 2012. Genomic selection for fruit quality traits in apple (*Malus × domestica* Borkh.). *PLoS ONE* **7**: e36674.

Kumar S, Garrick DJ, Bink MCAM, Whitworth C, Chagné D, Volz RK. 2013. Novel genomic approaches unravel genetic architecture of complex traits in apple. *BMC Genomics* **14**: 393.

Kumar S, Molloy C, Muñoz P, Daetwyler H, Chagné D, Volz R. 2015. Genome-enabled estimates of additive and nonadditive genetic variances and prediction of apple phenotypes across environments. *G3: Genes, Genomes, Genetics* **5**: 2711–2718.

Laloë D. 1993. Precision and information in linear models of genetic evaluation. *Genetics Selection Evolution* **25**: 557–576.

Lassois L, Denancé C, Ravon E, Guyader A, Guisnel R, Hibrand-Saint-Oyant L, Poncet C, Lasserre-Zuber P, Feugey L, Durel C-E. 2016. Genetic diversity, population structure, parentage analysis, and construction of core collections in the French apple germplasm based on SSR markers. *Plant Molecular Biology Reporter* **34**: 827–844.

Lê S, Josse J, Husson F. 2008. FactoMineR□: an R Package for multivariate analysis. *Journal of Statistical Software* **25**.

Lehner B. 2011. Molecular mechanisms of epistasis within and between genes. *Trends in Genetics* **27**: 323–331.

Longhi S, Hamblin MT, Trainotti L, Peace CP, Velasco R, Costa F. 2013. A candidate gene based approach validates Md-PG1 as the main responsible for a QTL impacting fruit texture in apple (*Malus × domestica* Borkh.). *BMC Plant Biology* **13**: 37.

Longhi S, Moretto M, Viola R, Velasco R, Costa F. 2012. Comprehensive QTL mapping survey dissects the complex fruit texture physiology in apple (*Malus × domestica* Borkh.). *Journal of Experimental Botany* **63**: 1107–1121.

Lorenz AJ, Smith KP. 2015. Adding genetically distant individuals to training populations reduces genomic prediction accuracy in barley. *Crop Science* **55**: 2657.

McClure KA, Gardner KM, Douglas GM, *et al.* 2018. A genome-wide association study of apple quality and scab resistance. *The Plant Genome* **11**.

McClure KA, Gong Y, Song J, *et al.* 2019. Genome-wide association studies in apple reveal loci of large effect controlling apple polyphenols. *Horticulture Research* **6**: 107.

McClure KA, Sawler J, Gardner KM, Money D, Myles S. 2014. Genomics: A potential panacea for the perennial problem. *American Journal of Botany* **101**: 1780–1790.

Meuwissen TH, Hayes BJ, Goddard ME. 2001. Prediction of total genetic value using genome-wide dense marker maps. *Genetics* **157**: 1819–29.

Migicovsky Z, Gardner KM, Money D, *et al.* 2016. Genome to phenome mapping in apple using historical data. *The Plant Genome* **9**.

Minamikawa MF, Nonaka K, Kaminuma E, *et al.* 2017. Genome-wide association study and genomic prediction in citrus: Potential of genomics-assisted breeding for fruit quality traits. *Scientific Reports* **7**: 1–13.

Minamikawa MF, Takada N, Terakami S, Saito T, Onogi A, Kajiya-Kanegae H, Hayashi T, Yamamoto T, Iwata H. 2018. Genome-wide association study and genomic prediction using parental and breeding populations of Japanese pear (*Pyrus pyrifolia* Nakai). *Scientific reports*, **8**: 11994.

Muranty H, Troggio M, Sadok I Ben, *et al.* 2015. Accuracy and responses of genomic selection on key traits in apple breeding. *Horticulture Research* **2**: 15060.

Peace CP, Bianco L, Troggio M, *et al.* 2019. Apple whole genome sequences: recent advances and new prospects. *Horticulture Research* **6**: 59.

R Core Team. 2014. R: A language and environment for statistical computing. R Foundation for Statistical Computing, Vienna, Austria. URL http://www.R-project.org/.

Rincent R, Laloë D, Nicolas S, *et al.* 2012. Maximizing the reliability of genomic selection by optimizing the calibration set of reference individuals: Comparison of methods in two diverse groups of maize inbreds (*Zea mays* L.). *Genetics* **192**: 715–728.

Rio S, Mary-Huard T, Moreau L, Charcosset A. 2019. Genomic selection efficiency and a priori estimation of accuracy in a structured dent maize panel. *Theoretical and Applied Genetics* **132**: 81–96.

Urrestarazu J, Denancé C, Ravon E, *et al.* 2016. Analysis of the genetic diversity and structure across a wide range of germplasm reveals prominent gene flow in apple at the European level. *BMC Plant Biology* **16**: 130.

Vanderzande S, Micheletti D, Troggio M, Davey MW, Keulemans J. 2017. Genetic diversity, population structure, and linkage disequilibrium of elite and local apple accessions from Belgium using the IRSC array. *Tree Genetics & Genomes* **13**: 125.

21

Warnes GR, Bolker B, Bonebakker L, *et al.* 2016. Package 'gplots': Various R programming tools for plotting data. R package version 2.17.0. URL https://CRAN.R-project.org/package=gplots

Wickham H. 2016. *ggplot2: elegant graphics for data analysis*. New York: Springer-Verlag.

Yang R-C. 1998. Estimating hierarchical F-statistics. *Evolution* **52**: 950.

Zhou Y, Isabel Vales M, Wang A, Zhang Z. 2016. Systematic bias of correlation coefficient may explain negative accuracy of genomic prediction. *Briefings in Bioinformatics* **18**: 44–753.

TABLES

Table 1. Description of the whole population and experimental design used for genomic prediction of texture. Maternal and paternal cultivars are given for full-sib biparental families. FEM, Foundation Edmund Mach; RCL, Research Center Laimburg. Cluster assignments as given by the discriminant analysis of principal components on 8,294 markers. Relationship to collection, mean additive relationship of progenies relative to collection.

Name	Mother	Father	Location	Evaluated years	# IDs	Cluster assignments (# IDs)						Relationship to collection
						1	2	3	4	5	6	
FjDe	Fuji	Delearly	FEM	2012-13	50	8	20	0	0	22	0	-0.056
FjPi	Fuji	Pinova	RCL	2012-14	70	1	30	0	0	39	0	-0.078
FjPL	Fuji	Pink Lady	FEM	2012-13	80	0	50	0	0	30	0	-0.071
GaPi	Royal Gala	Pinova	RCL	2012-14	36	0	0	0	0	36	0	-0.021
GaPL	Royal Gala	Pink Lady	RCL	2012-14	15	0	0	0	0	15	0	-0.020
GDFj	Golden Delicious	Fuji	RCL	2012-14	27	0	6	0	0	21	0	-0.057
Collection	-	-	FEM	2012-13-15	259	45	37	31	55	66	25	-

TABLES

Table 2. Summary of texture traits assessed in the whole population. h^2, broad sense heritability. For comparison, h^2 are also given considering measurements of the collection only.

Trait	Mean	SD	h^2	h^2 (COLL only)
ALD	5094	2049	0.938	0.928
ANP	50.4	39.1	0.924	0.909
APMax	65.2	4.38	0.921	0.880
APMean	49.6	3.12	0.951	0.915
Area	813	273	0.951	0.930
FF	10.1	3.98	0.946	0.929
FLD	101	5.78	0.955	0.937
Fmax	11.8	4.02	0.946	0.924
FMean	9.60	3.31	0.951	0.929
FNP	17.9	4.16	0.934	0.931
IF	9.94	3.29	0.933	0.906
YM	1.19	0.353	0.899	0.890

24

TABLES

Table 3. Maximum accuracies obtained among four training set optimization methods in predictions made for each combination of trait and family.

Family	Trait	Accuracy	TRS size	Method
FjDe	ALD	0.23	77	Mean relationship
FjDe	FNP	0.18	21	Max relationship
FjDe	PC1	0.26	77	Mean relationship
FjDe	PC2	0.36	56	Max relationship
FjPi	ALD	0.36	189	Mean relationship
FjPi	FNP	0.59	174	Max relationship
FjPi	PC1	0.36	178	Max relationship
FjPi	PC2	0.26	202	Mean relationship
FjPL	ALD	0.10	130	CDmean-opt
FjPL	FNP	0.16	22	Max relationship
FjPL	PC1	0.20	120	Max relationship
FjPL	PC2	0.22	10	CDmean-opt
GaPi	ALD	0.46	156	Mean relationship
GaPi	FNP	0.40	13	Max relationship
GaPi	PC1	0.54	191	Clusters
GaPi	PC2	0.28	19	Mean relationship
GaPL	ALD	0.72	136	Clusters
GaPL	FNP	0.78	37	Max relationship
GaPL	PC1	0.81	129	Mean relationship
GaPL	PC2	0.40	140	Max relationship
GDFj	ALD	0.21	66	Mean relationship
GDFj	FNP	0.32	15	Max relationship
GDFj	PC1	0.19	31	Mean relationship
GDFj	PC2	0.01	10	Mean relationship

25

FIGURE LEGENDS

Figure 1. Principal component analysis (PCA) of 12 texture sub-traits. A, PCA 2D-plot of variables, with acoustic traits in blue and mechanical traits in red with 1, ANP; 2, ALD; 3, APMAx; 4, APMean; 5, FNP; 6, FLD; 7,FF; 8, YM; 9, Area; 10; Fmean; 11, Fmax; 12, IF. B, PCA 2D-plot of individuals with collection individuals represented as dots and families as ellipses. C, PCA 2D-plot of individuals showing family offspring and their respective parents.

Figure 2: Realized additive relationship calculated with 8,294 SNPs. Families indicated in black with brackets and parents are indicated in red.

Figure 3: Discriminant analysis of principal components and cluster assignments of individuals based on 8,294 SNPs. A, projection on principal component (PC) 1 and 3 of the cluster assignments of individuals in the collection with parents of families indicated with their names. Black lines materialize the PCs defining clusters. B, Predicted cluster assignments of progenies of the six full-sib families projected on PC1 and PC3 axes and represented by dots, with collection individuals in the six genetic clusters represented as ellipses (same color legend as in part A). C, Distribution of individuals across the six genetic clusters in each population.

Figure 4: Mean and standard deviation of accuracies obtained in three prediction scenarios. In scenario 1, each family was predicted using the collection only. In scenario 2, 30% of individuals of the predicted family were added to the collection in the TRS and the remaining 70% formed the TS. In scenario 3, a single half-sib family was added to the collection to form the TRS. The predictions were made with model A, which does not take into account the genetic clustering of individuals.

Figure 5: Optimization of the training population for the prediction of each family using *a priori* information on individuals. A, addition of individuals in the TRS by decreasing mean relatedness to the predicted family; B, addition of individuals in the TRS by decreasing maximum relatedness to the predicted family; C, addition of clusters by decreasing mean relatedness to the predicted family; D, selection of individuals for TRS of different sizes based on the five principal components obtained with discriminant analysis of principal components and using the CDmean design criteria. The color legend applies for all parts of the figure.
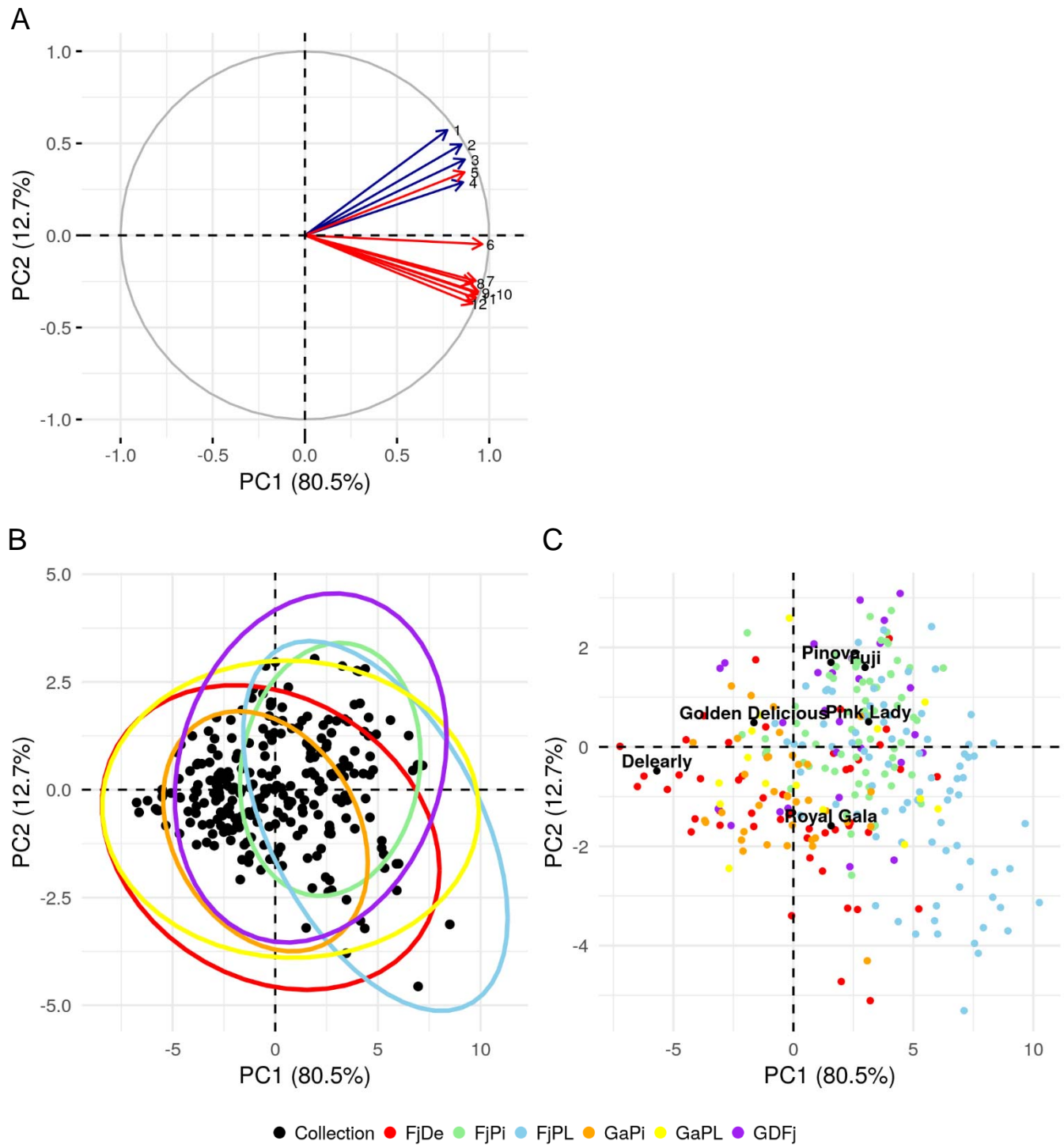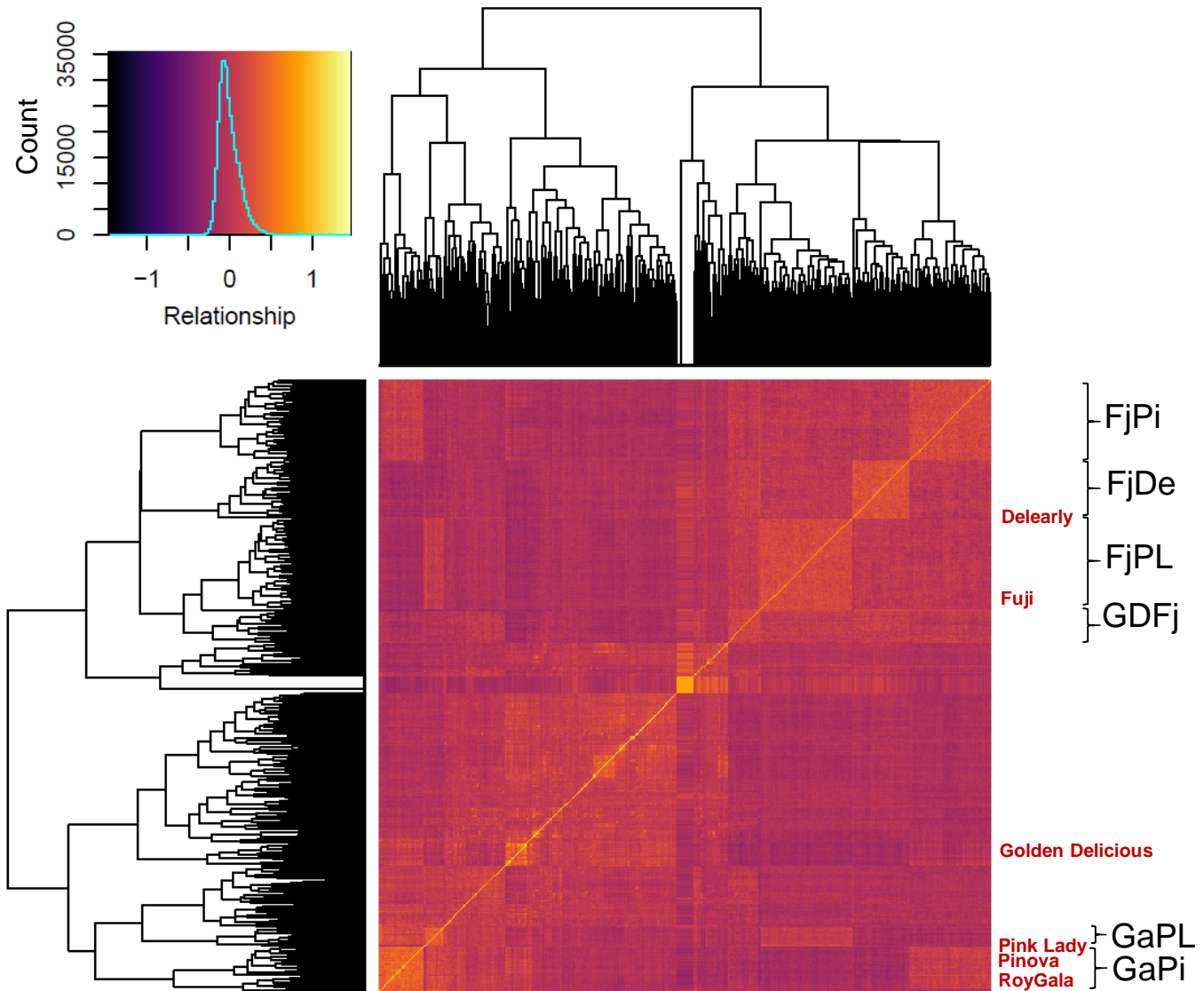
FIGURE 1

FIGURE 2

Figure 2: Realized additive relationship calculated with 8,294 SNPs. Families indicated in black with brackets and parents are indicated in red.
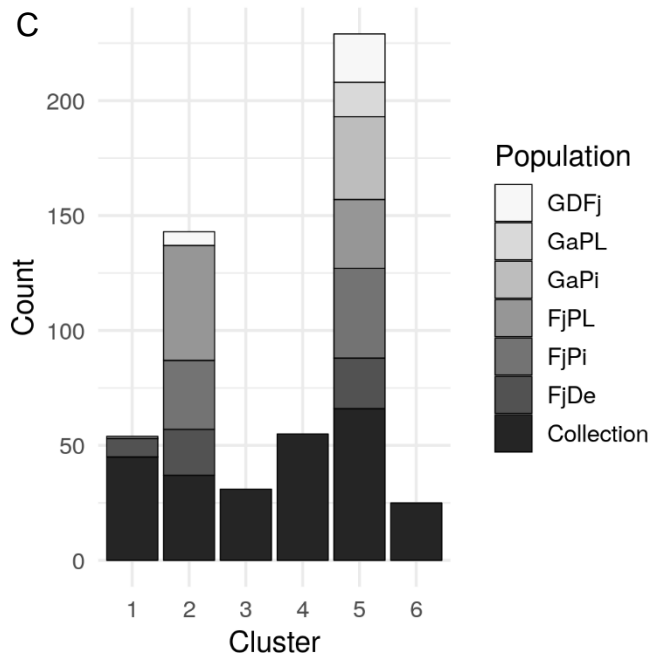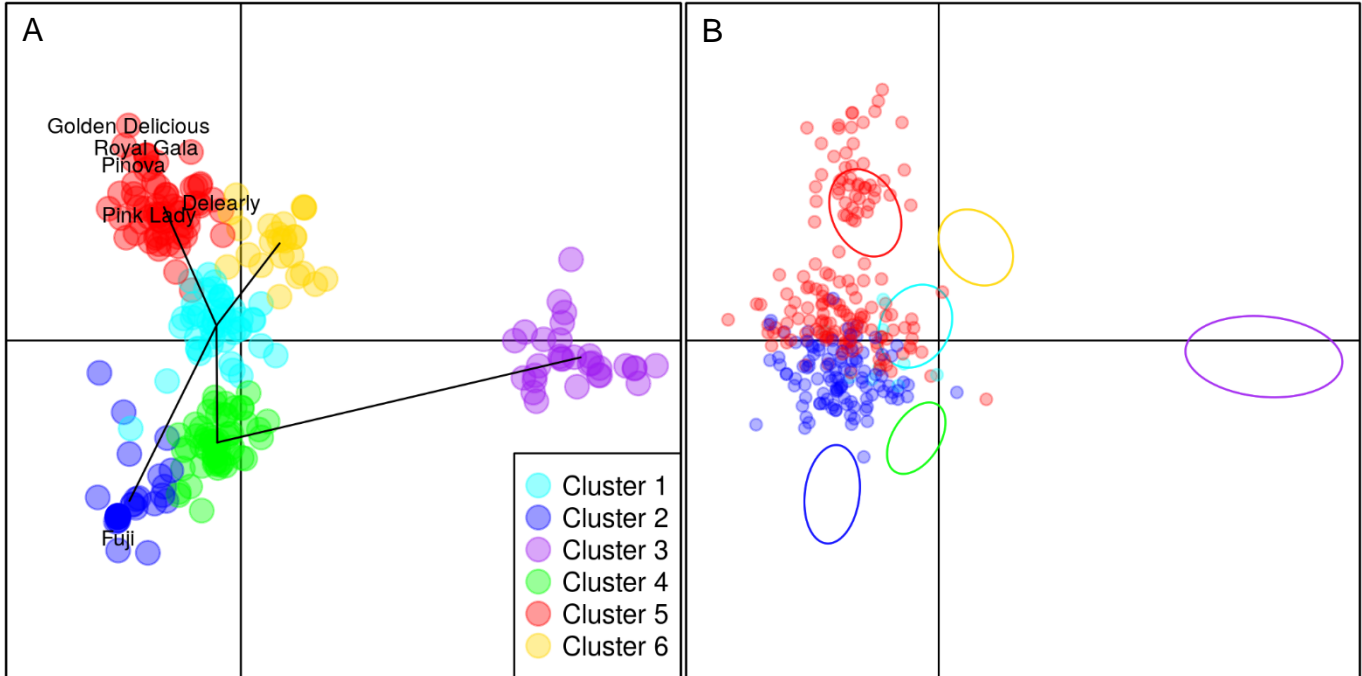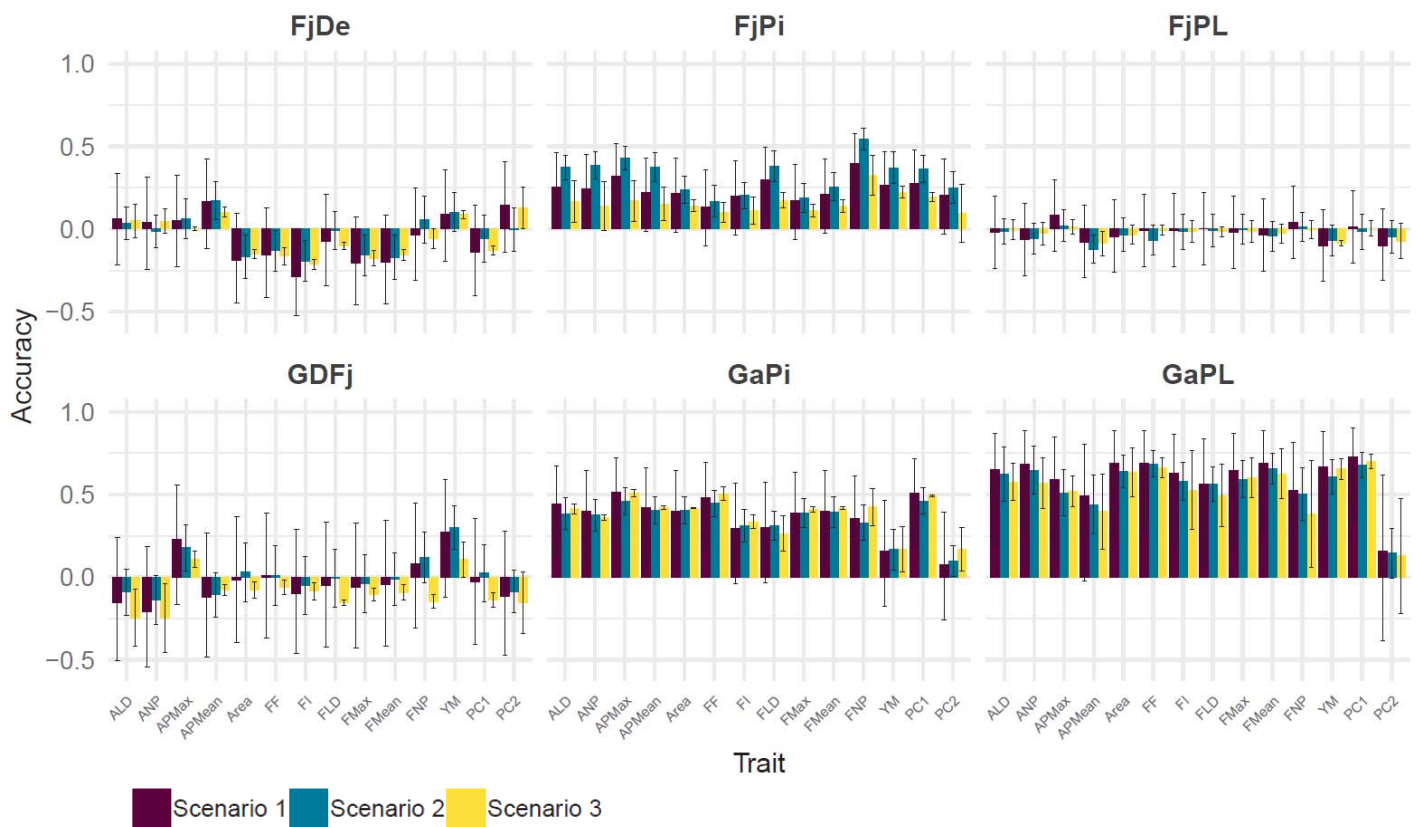
FIGURE 3

FIGURE 4

FIGURE 5